Soft Matter

COMMUNICATION

View Article Online
View Journal

Check for updates

Cite this: DOI: 10.1039/d4sm01542h

Received 30th December 2024,
Accepted 26th January 2025

DOI: 10.1039/d4sm01542h

rsc.li/soft-matter-journal

Published on 27 January 2025. Downloaded by Fudan University on 2/6/2025 5:34:41 AM.

Fluorescence-switching 2-D sheet structure formed by self-assembly of cruciform aromatic amphiphiles†

Wei Zhang,[ab] Yongsheng Li,[b] Tianyi Zheng,[b] Ying Xie,*[a] Xianyin Dai[bc] and Myongsoo Lee*[b]

We report that aromatic amphiphiles based on cruciform aromatic segments self-assemble into 2-D sheet structures in aqueous environments. Notably, the aromatic amphiphile based on a pyrene unit generates fluorescence-switching 2-D sheet structures. In a pH-neutral condition, the sheets show strong excimer emission. However, upon lowering the pH the excimer emission is quenched due to loosely-packed pyrene units. Subsequent return of pH to a neutral condition leads to full recovery of the excimer emission, indicative of fully-reversible fluorescence emission switching.

Introduction

The development of self-assembled nanostructures using amphiphilic aromatic molecules has garnered considerable attention due to their potential in bioactive materials and nanomaterials.[1–6] Rationally designing the molecular shape and controlling the relative volume fraction of amphiphilic aromatic molecules can give rise to a variety of the well-defined supramolecular structures. Especially, in the case of rigid-flexible block molecules, the large difference in stiffness between the rigid aromatic segments and the flexible hydrophilic coil segments drives the formation of a variety of supramolecular structures, including vesicles, networks, and tubules in aqueous solutions.[7–10] Among various supramolecular structures, a 2-D flat sheet structure is particularly attractive because the 2-D assembly is able to perform various unique functions that are not, in many cases, observed in the other supramolecular structures.[11–16] For example, self-assembled flat ribbons, which are composed of laterally assembled primary 1-D nanofiber structures, transform into scrolled tubules in response to carbohydrate.[17] As a result, the planar sheet structures are able to encapsulate carbohydrate molecules by spontaneous rolling into tubules containing each an internal hollow cavity. In addition, we have demonstrated that planar sheet structures are able to become spontaneously curved to form hollow vesicles by budding in response to a curved guest such as coronene.[18] We have also reported static and dynamic nanosheets formed from selective self-assembly of non-planar aromatic macrocycles based on anthracene units.[19] A solution including a mixture of the two isomers exhibits self-sorting behavior, generating two co-present independent self-assembled structures, namely the planar sheets and the folded scrolls. Another approach to construct planar sheet structures includes the lateral assembly of helical nanofibers that provide chiral void spaces. For example, helical peptides grafted laterally can be aligned parallel to one another to form planar sheet structures.[20,21] Considering the parallel arrangements of the helical peptides, the internal cavities formed between the helical peptide arrangements can, due to preferred interactions, discriminate one enantiomer from a solution of a racemic mixture. We have also reported that planar aromatic amphiphiles can generate, in aqueous solution, flat 2-D structures able to function as highly efficient enantiomer-separating membranes, displaying fluorescence sensing characteristics.[22] As an extension of our efforts to create flat 2-D sheet structures capable of performing unique functions, we designed aromatic amphiphiles based on optically-active aromatic segments. The designed molecules contain hydrophilic dendrons at opposite ends of the aromatic portion; thus aromatic amphiphiles with symmetrically-grafted dendrons drive self-assembly into a 2-D sheet structure displaying no curvature, as reported previously in our laboratory.[19,22,23] In particular, pyrene-based planar aromatic molecules exhibit interesting fluorescence properties due to their efficient excimer formation?[24–28] Such excimer fluorescence emissions occur in the vicinity of ~480 nm as a broad band as compared

[a] College of Science, Shenyang University of Chemical Technology, Liaoning 110142, China. E-mail: xieying.72@163.com
[b] Department of Chemistry, State Key Lab of Molecular Engineering of Polymers, and Shanghai Key Lab of Molecular Catalysis and Innovative Materials, Fudan University, Shanghai 200438, China. E-mail: mslee@fudan.edu.cn
[c] School of Chemistry and Pharmaceutical Engineering, Shandong First Medical University & Shandong Academy of Medical Sciences, Taian, 271016, China

† Electronic supplementary information (ESI) available. See DOI: https://doi.org/10.1039/d4sm01542h

Published on 27 January 2025. Downloaded by Fudan University on 2/6/2025 5:34:41 AM.

to well-structured monomer emission at about 375–400 nm. Therefore, the incorporation of an optically-active pyrene unit into a self-assembly including pyridine would endow the supramolecular structure with switchable fluorescence properties, with the switching triggered by a change in pH.[29,30] Here, we report switchable 2-D sheet structures formed from the self-assembly of a cruciform aromatic amphiphile in aqueous environments. The aromatic amphiphiles generate ~3-nm-thick 2-D nanosheet structures. Notably, the sheet structure based on a pyrene unit undergoes reversible fluorescence switching in response to a pH change.

Results and discussion

The molecules forming single-layer planar sheet structures consisting of a cruciform aromatic segment and oligoether dendrons grafted at opposite sides of the aromatic plane were synthesized in a stepwise manner according to the procedures described in ESI† (Scheme 1).

The resulting amphiphilic molecules were characterized using ^{1}H- and ^{13}C-NMR spectroscopy, and LC mass spectroscopy, the results of which were shown to be in full agreement with the chemical structures presented. The cruciform aromatic amphiphiles can, due to their amphiphilic characteristics, form supramolecular assemblies in solvents selected for the hydrophilic flexible dendrons.[31] To investigate the self-aggregation behavior of **1**, we subjected it (at a concentration to 0.01%) to UV-Vis and fluorescence spectroscopy analyses. Inspection of the absorption of the aromatic amphiphile in aqueous solution showed a hypochromic effect with respect to that recorded in $CHCl_3$, and a quenching of the fluorescence (Fig. 1a and b), indicative of self-assembly.[23] The formation of self-assembled nanostructures of the aromatic amphiphile **1** in aqueous solution was investigated using transmission electron microscopy (TEM) and atomic force microscopy (AFM). The TEM image showed flat 2-D sheet structures with uniform sheet thickness (Fig. 1c). Closer examination of the images showed a sheet consisting of longitudinal stripes with a regular spacing of ~3 nm (Fig. 1c, inset), demonstrating the sheet assembly having originated from the lateral association of

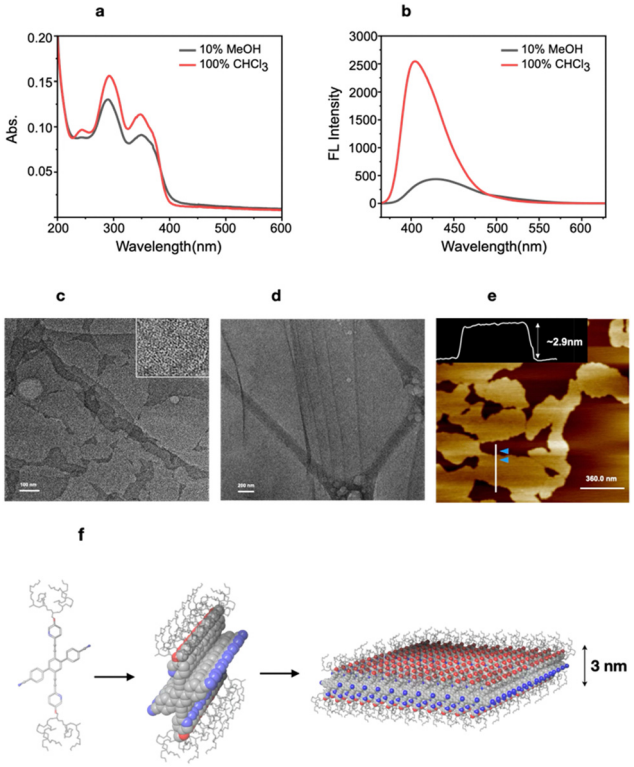

Fig. 1 (a) and (b) UV-Vis and fluorescence spectra of **1** (50 μM) in MeOH/H_2O (1 : 9 v/v) and 100% $CHCl_3$; (c) TEM image of **1** (25 μM) in MeOH/H_2O (3 : 17 v/v); (d) cryo-TEM image of **1** (25 μM) in MeOH/H_2O (3 : 17 v/v); (e) AFM image of **1** (25 μM) in MeOH/H_2O (3 : 17 v/v); (f) depiction of the single-layered sheet structure of **1**.

preformed fibrils. The formation of the planar sheet nanostructures was further confirmed using cryogenic TEM (cryo-TEM) with a vitrified aqueous solution, with the results here providing further evidence of the aggregates existing as flat 2-D sheets in bulk solution (Fig. 1d). Additional structural information for the sheets was obtained by taking atomic force microscopy (AFM) measurements of **1** on a hydrophilic mica substrate in a completely dried state. The corresponding AFM image revealed single-layered planar sheets each with a thickness of 3.0 nm, consistent with the molecular dimensions of **1** (Fig. 1e). These results demonstrated

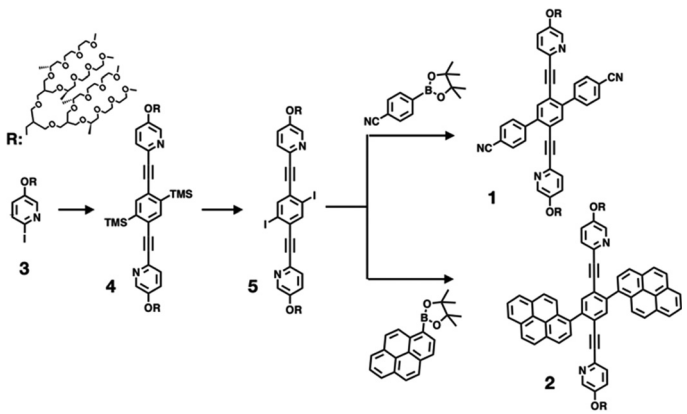

Scheme 1 Synthesis of amphiphilic molecules **1** and **2**.

This journal is © The Royal Society of Chemistry 2025

Published on 27 January 2025. Downloaded by Fudan University on 2/6/2025 5:34:41 AM.

the ability of the cruciform aromatic amphiphile in aqueous solution to self-assemble into stable, single-layered 2-D sheet structures through lateral association of primary fibrils (Fig. 1f).

Replacing the cyanophenyl group in the aromatic amphiphile with a pyrene capable of excimer formation would be expected to endow the pyridine-based 2-D sheet structure with a pH-responsive fluorescence property because the excimer packing of the pyrene units would be changed with the protonation of the pyridine unit.[28] Indeed, the amphiphilic molecule (**2**) based on pyrene showed strong fluorescence at the wavelength range of 420 nm to 570 nm in an aqueous methanol solution (9/1 v/v) with a lack of any vibronic feature in the emission band (Fig. 2a). This result demonstrated the self-assembly of **2** being followed by excimer formation of the pyrene units in the self-assembly.[26] TEM investigations revealed the formation of flat 2-D sheet structures ~3-nm-diameter lateral stripes (Fig. 2b). The formation of a single-layered 2-D sheet structures in bulk solution was further confirmed using cryo-TEM (Fig. 2c). The AFM image of **2** showed 3.0-nm-thick single-layered planar sheets (Fig. 2d), similar to that of **1**. In combination with the excimer formation in the self-assembled state, these results indicated the pyrene units of adjacent molecules to be sufficiently close to each other in the 2-D sheet self-assembly to form pyrene excimers.

Considering that the emission of pyrene excimers is very sensitive to the local environment,[27,28] we envisioned that the sheet structures with strong excimer emission would display pH sensitivity due to the pyridine units in the aromatic portion. In the neutral condition (pH = 7), the hydrophobic and conjugated pyrene moieties have been previously shown to stack closely together through strong aromatic interactions, with this close stacking responsible for the strong emission of the pyrene excimers formed under these conditions.[22] However, adding an equimolar amount of HCl into the aqueous solution of **2** yielded considerable quenching of the fluorescence emission

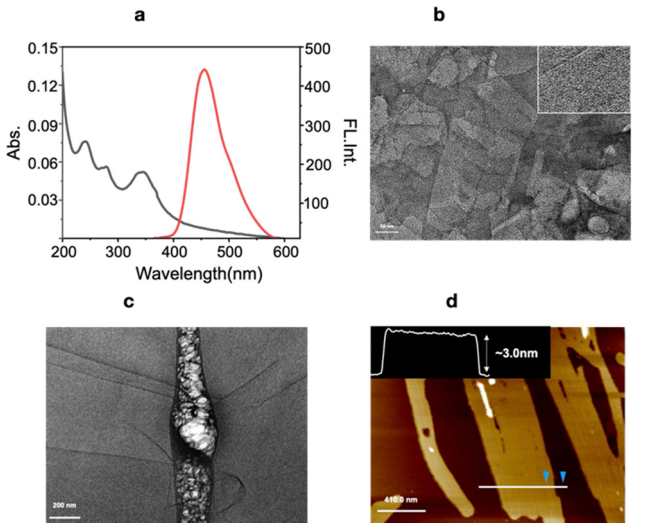

Fig. 2 (a) UV-Vis and fluorescence spectra of **2** (50 μM) in MeOH/H_2O (1 : 9 v/v); (b) TEM image of **2** (25 μM) in MeOH/H_2O (3 : 17 v/v); (c) cryo-TEM image of **2** (25 μM) in MeOH/H_2O (3 : 17 v/v); (d) AFM image of **2** (25 μM) in MeOH/H_2O (3 : 17 v/v).

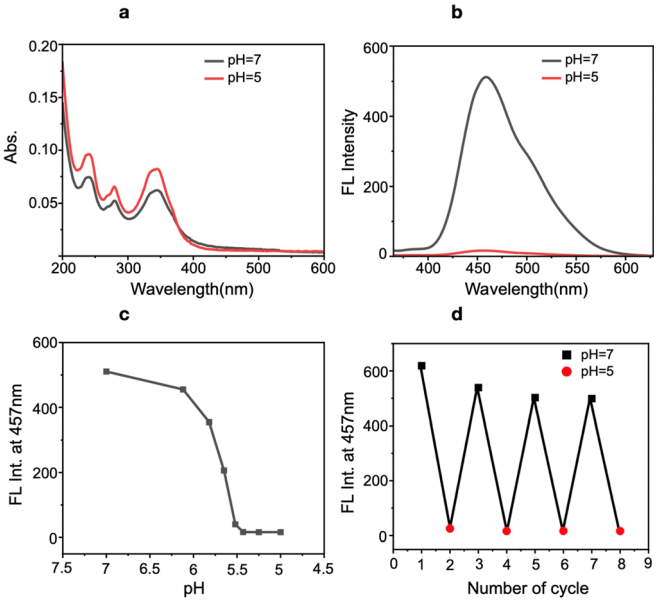

Fig. 3 (a) and (b) UV-Vis and fluorescence spectra of **2** (50 μM) in MeOH/H_2O (1 : 9 v/v) with pH = 5 and pH = 7; (c) plot showing fluorescence intensity of **2** decreasing with acidity increasing; (d) plot showing reversible induction of emission intensity with cycling between pH = 7 and pH = 5.

at ~480 nm followed by an increase in UV absorption with respect to the neutral solution without sacrificing its intact 2-D self-assembled structure (Fig. 3a and b). The emission intensity at 480 nm was observed to decrease abruptly with decreasing pH and then level off at pH = 5 (Fig. 3c), demonstrating the fluorescence emission of the sheet structure of **2** to be very sensitive to a small change in pH. We attributed the fluorescence quenching to the pyrene units becoming more loosely packed upon lowering the pH, as reflected in the intensity increase of the UV absorption (hyperchromic effect) with respect to the neutral solution. As a result of the protonation of the pyridine units in the aromatic portions loosening the pyrene packing due to repulsive interactions between adjacent pyridinium cations, the sheet solution exhibited a decrease in the intensity of the excimer emission upon lowering of the pH (Fig. 4). This result demonstrated that the fluorescence of the sheet structure can be controlled by adjusting the pH to control the intermolecular interactions in the self-assembled state. When the solution was neutralized by adding NaOH to it, a restoration of strong fluorescence emission was observed, indicative of the sheets having undergone reversible fluorescence switching between neutral and acidic conditions (Fig. 3d). The reversibility of the fluorescence response signal of the sheet of **2** between a pH of 7 and 5 was further investigated. As shown in Fig. 3d, cycling of the pH-dependent fluorescence signal conversion can occur at least four times, indicative of the sheet solution displaying full reversibility in fluorescence switching triggered by a pH change. Compared to **1**, which was shown not to display excimer emission (Fig. S11, ESI†), **2** was found to be very sensitive to a change in packing due to excimer formation; thus, incorporation of a pyrene unit into a self-assembly can be concluded to provide new avenues toward fluorescence-switching 2-D materials.

Published on 27 January 2025. Downloaded by Fudan University on 2/6/2025 5:34:41 AM.

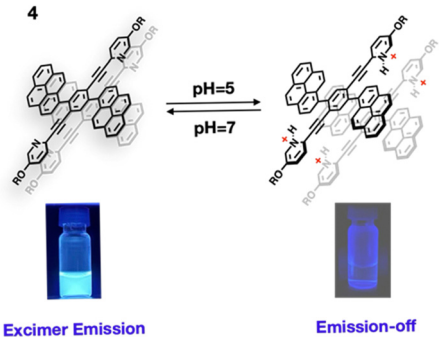

Fig. 4 Schematic representation of fluorescence emission on/off switching mechanism.

These experiments have demonstrated the ability of the 2-D sheet based on a pyrene unit to undergo fluorescence switching consecutively in response to a small pH change; thus the self-assembled sheets can be used as a promising fluorescence sensor for detecting acidic substances in aqueous environments.

Conclusions

We synthesized aromatic amphiphiles consisting of a cruciform aromatic segment and hydrophilic dendrimers. The amphiphilic molecules self-assemble into flat sheet structures in aqueous environments. The sheet structures based on pyrene units show strong excimer emission at pH 7 but weak such emission at pH 5. The dynamic switching behavior of the sheets is attributed to changes in the packing of pyrene aromatic segments upon changing the pH. This unique fluorescence switching response to external stimuli might provide a new strategy for rational designing and synthesizing supramolecular materials that in aqueous solutions can sense such stimuli.

Author contributions

W. Z. and Y. L. synthesized molecules. W. Z. performed spectroscopic measurements. W. Z., T. Z. and X. D. performed TEM, cryo-TEM and AFM experiments. M. L. developed the concept, M. L. and Y. X. supervised the research, and M. L. wrote the manuscript with input from all authors.

Data availability

The data supporting this article have been included as part of the ESI.†

Conflicts of interest

The authors declare no competing interests.

Acknowledgements

This work was supported by National Natural Science Foundation of China (Grant No. 92156023, 92356306, and 22150710515).

References

1 A. J. S. I. Stupp, *Curr. Opin. Colloid Interface Sci.*, 1998, **3**, 20–26.
2 M. Lee, B.-K. Cho and W.-C. Zin, *Chem. Rev.*, 2001, **101**, 3869–3892.
3 M. He, F. Qiu and Z. Lin, *J. Mater. Chem.*, 2011, **21**, 17039–17048.
4 C.-L. Liu, C.-H. Lin, C.-C. Kuo, S.-T. Lin and W.-C. Chen, *Prog. Polym. Sci.*, 2011, **36**, 603–637.
5 Y.-b Lim, K. S. Moon and M. Lee, *J. Mater. Chem.*, 2008, **18**, 2909–2918.
6 J. Zhang, X.-F. Chen, H.-B. Wei and X.-H. Wan, *Chem. Soc. Rev.*, 2013, **42**, 9127–9154.
7 J. H. Ryu, D. J. Hong and M. Lee, *Chem. Commun.*, 2008, 1043–1054.
8 X. Gou, H. Y. Zhao, Z. Huang, Y. Yang and L. Y. Jin, *Langmuir*, 2024, **40**, 7106–7113.
9 H.-J. Kim, T. Kim and M. Lee, *Acc. Chem. Res.*, 2011, **44**, 72–82.
10 Y. Kim, W. Li, S. Shin and M. Lee, *Acc. Chem. Res.*, 2013, **46**, 2888–2897.
11 Z. Sun, T. Liao, Y. Dou, S. M. Hwang, M.-S. Park, L. Jiang, J. H. Kim and S. X. Dou, *Nat. Commun.*, 2014, **5**, 3813.
12 J.-K. Kim, E. Lee, Y.-H. Jeong, J.-K. Lee, W.-C. Zin and M. Lee, *J. Am. Chem. Soc.*, 2007, **129**, 6082–6083.
13 B. Shen, Y. Kim and M. Lee, *Adv. Mater.*, 2020, **32**, 1905669.
14 J. W. Colson and W. R. Dichtel, *Nat. Chem.*, 2013, **5**, 453–465.
15 M. J. Kory, M. Wörle, T. Weber, P. Payamyar, S. W. van de Poll, J. Dshemuchadse, N. Trapp and A. D. Schlüter, *Nat. Chem.*, 2014, **6**, 779–784.
16 C. M. Atienza and L. Sánchez, *Chem. – Eur. J.*, 2024, **30**, e202400379.
17 B. Shen, Y. He, Y. Kim, Y. Wang and M. Lee, *Angew. Chem., Int. Ed.*, 2016, **55**, 2382–2386.
18 Y. Kim and M. Lee, *Chem. – Eur. J.*, 2015, **21**, 5736–5740.
19 Y. Wang, Y. Kim and M. Lee, *Angew. Chem., Int. Ed.*, 2016, **55**, 13122–13126.
20 X. Chen, Y. He, Y. Kim and M. Lee, *J. Am. Chem. Soc.*, 2016, **138**, 5773–5776.
21 X. Chen, Y. Wang, H. Wang, Y. Kim and M. Lee, *Chem. Commun.*, 2017, **53**, 10958–10961.
22 Y. Wang and M. Lee, *ChemPlusChem*, 2020, **85**, 711–714.
23 Y. Wang, X. Feng and M. Lee, *Org. Chem. Front.*, 2021, **8**, 3681–3685.
24 H. J. Kim, M. H. Lee, L. Mutihac, J. Vicens and J. S. Kim, *Chem. Soc. Rev.*, 2012, **41**, 1173–1190.
25 D. T. Quang and J. S. Kim, *Chem. Rev.*, 2010, **110**, 6280–6301.
26 R. Chopra, P. Kaur and K. Singh, *Anal. Chim. Acta*, 2015, **864**, 55–63.
27 T. Liu, Z. Huang, R. Feng, Z. Ou, S. Wang, L. Yang and L. J. Ma, *Dyes Pigment.*, 2020, **174**, 108102.
28 Y. Zhao, P. Xu, K. Zhang, H. Schönherr and B. Song, *Cell Rep. Phys. Sci.*, 2022, **3**, 100734.
29 Y. Kim, H. Li, Y. He, X. Chen, X. Ma and M. Lee, *Nat. Nanotechnol.*, 2017, **12**, 551–556.
30 H. Wang, Y. Wang, B. Shen, X. Liu and M. Lee, *J. Am. Chem. Soc.*, 2019, **141**, 4182–4185.
31 L. Tan, M. Sun, H. Wang, J. Wang, J. Kim and M. Lee, *Nat. Synth.*, 2023, **2**, 1222–1231.

 This journal is © The Royal Society of Chemistry 2025